Developmental Biology 324 (2008) 41–54

Contents lists available at ScienceDirect

Developmental Biology

journal homepage: www.elsevier.com/developmentalbiology

Regulation of neurocoel morphogenesis by Pard6γb

Chantilly Munson [a], Jan Huisken [a], Nana Bit-Avragim [b,c], Taiyi Kuo [a], P.D. Dong [a], Elke A. Ober [a,1], Heather Verkade [a,2], Salim Abdelilah-Seyfried [b], Didier Y.R. Stainier [a,*]

[a] Department of Biochemistry and Biophysics, Programs in Developmental Biology, Genetics and Human Genetics, University of California, San Francisco, San Francisco, CA 94158, USA
[b] Max Delbrück Center (MDC) for Molecular Medicine, Robert-Rössle Strasse 10, 13125 Berlin, Germany
[c] The Charité, Department of Cardiology, Campus Buch and Campus Virchow Clinics, Humboldt University, Berlin, Germany

ARTICLE INFO

Article history:
Received for publication 20 May 2008
Revised 16 August 2008
Accepted 23 August 2008
Available online 9 September 2008

Keywords:
Par6
Neurulation
Apicobasal polarity
Epithelium
Zebrafish

ABSTRACT

The Par3/Par6/aPKC protein complex plays a key role in the establishment and maintenance of apicobasal polarity, a cellular characteristic essential for tissue and organ morphogenesis, differentiation and homeostasis. During a forward genetic screen for liver and pancreas mutants, we identified a *pard6γb* mutant, representing the first known *pard6* mutant in a vertebrate organism. *pard6γb* mutants exhibit defects in epithelial tissue development as well as multiple lumens in the neural tube. Analyses of the cells lining the neural tube cavity, or neurocoel, in wildtype and *pard6γb* mutant embryos show that lack of Pard6γb function leads to defects in mitotic spindle orientation during neurulation. We also found that the PB1 (aPKC-binding) and CRIB (Cdc-42-binding) domains and the KPLG amino acid sequence within the PDZ domain (Pals1-and Crumbs binding) are not required for Pard6γb localization but are essential for its function in neurocoel morphogenesis. Apical membranes are reduced, but not completely absent, in mutants lacking the zygotic, or both the maternal and zygotic, function of *pard6γb,* leading us to examine the localization and function of the three additional zebrafish Pard6 proteins. We found that Pard6α, but not Pard6β or Pard6γa, could partially rescue the *pard6γb*^{s441} mutant phenotypes. Altogether, these data indicate a previously unappreciated functional diversity and complexity within the vertebrate *pard6* gene family.

Introduction

Cell polarization distributes cellular constituents into discrete domains and results in asymmetric distribution of cellular activity. Three main protein complexes (Par3/Par6/aPKC, Crumbs/Discs lost/Stardust and Lethal giant larvae/Discs large/Scribble) regulate apicobasal polarity by localizing or restricting tight junction proteins toward the apical end of lateral membranes and by organizing the cytoskeleton (reviewed by Gibson and Perrimon, 2003). Epithelial cells exhibit apicobasal polarity, which allows the establishment of physiological barriers (reviewed by Rodriguez-Boulan and Nelson, 1989). Formation of polarized epithelial sheets is also essential for cellular and tissue morphogenesis, movement, and differentiation during metazoan development (reviewed by Gibson and Perrimon, 2003).

Forward genetic screens in zebrafish (*Danio rerio*) have identified embryonic lethal mutations in several genes that regulate epithelial development including *heart and soul* (*has/prkci*, previously known as *apkcλ*) (Horne-Badovinac et al., 2001; Peterson et al., 2001), *nagie oko* (*nok/pals1/mpp5*) (Wei and Malicki, 2002), *oko meduzy* (*ome/crb2*) (Omori and Malicki, 2006), and *mosaic eyes* (*moe/epb41l5*) (Jensen and Westerfield, 2004). Each of these mutations causes defects in heart tube assembly, retinal pigmented epithelium development, inflation of the brain ventricles, and body curvature. Further analyses have revealed distinct roles for each of these genes in different aspects of developing organs derived from epithelia (Horne-Badovinac et al., 2003; Kramer-Zucker et al., 2005; Omori and Malicki, 2006; Rohr et al., 2006; Bit-Avragim et al., 2008b; Christensen and Jensen, 2008). For example, zygotic expression of *has/prkci* and *nok/mpp5* appears to regulate distinct aspects of heart development (Rohr et al., 2006) and *ome/crb2* regulates the elongation of cilia (Omori and Malicki, 2006).

The *has/prkci* mutation affects one member of the Par3/Par6/aPKC complex. Studies in the *C. elegans* zygote first identified the components of this complex as essential for asymmetric cell division (Etemad-Moghadam et al., 1995; Guo and Kemphues, 1995; Watts et al., 1996). Since then, the influence of this complex on polarization and development has expanded to include *Drosophila* embryos and mammalian cells (Suzuki and Ohno, 2006). Analysis of zebrafish *has/prkci* mutants (Horne-Badovinac et al., 2001; Peterson et al., 2001), as well as *pard3* morpholino injected embryos, aka morphants, (Geldmacher-Voss et al., 2003; Wei et al., 2004) and *Pard3* deficient mice (Hirose et al., 2006) has increased our understanding of how these proteins regulate the complex events of vertebrate organo-

* Corresponding author.
E-mail address: didier_stainier@biochem.ucsf.edu (D.Y.R. Stainier).
[1] Current address: National Institute for Medical Research, Division of Developmental Biology, The Ridgeway, London, NW7 1AA, UK.
[2] Current address: School of Biological Sciences, Monash University, Clayton, VIC 3800, Australia.

0012-1606/$ – see front matter © 2008 Elsevier Inc. All rights reserved.
doi:10.1016/j.ydbio.2008.08.033

genesis. However, the role of Par6 during vertebrate development has remained elusive.

The ability of Par6 to polarize epithelial cells depends on at least four protein-protein interactions mediated through three domains. Par6 interacts with aPKC/Prkci through its *P*hox and *B*em*1*p (PB1) domain (Suzuki et al., 2001; Suzuki et al., 2003), with Cdc42 through its partial *C*dc42/*R*ac *i*nteractive *b*inding (CRIB) domain (Joberty et al., 2000; Lin et al., 2000; Qiu et al., 2000; Garrard et al., 2003; Hutterer et al., 2004), and with both PAR-3/Pard3 (Joberty et al., 2000; Lin et al., 2000) and Pals1/Mpp5 (Hurd et al., 2003; Wang et al., 2004) through its PDZ (*P*SD-95/*D*lg/*Z*O-1) domain. Only one Par6 protein exists in *C. elegans* and *Drosophila*, but a family of three proteins is present in mammals: Pard6A, Pard6B, and Pard6G (Joberty et al., 2000). Studies in MDCK cells have suggested that these different family members exhibit different subcellular localization and have distinct functions (Gao and Macara, 2004). However, there has been no *in vivo* analysis of the different vertebrate Pard6 family members during development.

Through neurulation, the neuroepithelium gives rise to the eyes, the brain and its ventricles, and the spinal cord. Many of these structures are disrupted in zebrafish embryos carrying mutations affecting apicobasal polarity (Horne-Badovinac et al., 2001; Wei and Malicki, 2002; Jensen and Westerfield, 2004; Lowery and Sive, 2005; Omori and Malicki, 2006). In zebrafish, the neuroepithelium begins as an epithelial-like structure at the neural plate stage, although it lacks polarized localization of apicobasal polarity markers (Papan and Campos-Ortega, 1999; Lowery and Sive, 2004; Ciruna et al., 2006). This neural plate converges to the midline and extends during somitogenesis to form the neural keel, a process that has the hallmarks of primary neurulation (Geldmacher-Voss et al., 2003; Lowery and Sive, 2004; Hong and Brewster, 2006). During this morphogenetic process, cells divide perpendicular to, and across, the midline (Geldmacher-Voss et al., 2003; Ciruna et al., 2006; Tawk et al., 2007). After the 12-somite stage (13 h post fertilization (hpf)), Pard3 forms foci of polarity along the midline of the neural keel (Geldmacher-Voss et al., 2003; Tawk et al., 2007). These foci continue to assemble (Tawk et al., 2007) and by approximately 21 hpf delineate continuous apical membranes and a slit lumen (Geldmacher-Voss et al., 2003). Following formation of these continuous apical membranes, fluid is pumped into the neurocoel and the brain ventricles inflate (Lowery and Sive, 2005). Coincident with the formation of the apical membranes, the mitotic spindles in dividing neuroepithelial cells rotate such that divisions now occur parallel to the plane of the midline (Geldmacher-Voss et al., 2003).

Several molecules implicated in vertebrate neurulation are components of the planar cell polarity or apicobasal polarity pathways (Ueno and Greene, 2003; Gotz and Huttner, 2005). Analysis of these molecular pathways in vertebrates is beginning to shed light on how the neural tube forms. The zebrafish provides a vertebrate genetic model that is amenable to live imaging and, therefore, offers distinct advantages for studying neurulation *in vivo*.

Here we report the identification of a mutation in the zebrafish *pard6γb* gene and analyze the resulting phenotype. *pard6γb* mutants show defects in the development of several epithelial tissues similar to *has/prkci* mutants (Horne-Badovinac et al., 2001; Peterson et al., 2001; Horne-Badovinac et al., 2003). Furthermore, they exhibit multiple lumens in the neural tube, a previously undescribed phenotype (Belting and Affolter, 2007). The Par3/Par6/aPKC(Prkci) complex has been suggested to affect orientation of the mitotic spindle in the neural tube stage (Geldmacher-Voss et al., 2003; von Trotha et al., 2006), and we show that *pard6γb* mutants exhibit defects in mitotic spindle orientation in the forming neural tube. Additional studies indicate that Pard6α, but not Pard6β or Pard6γa, could partially rescue the *pard6γb*^{s441} mutant phenotypes, thereby revealing a previously unappreciated functional diversity and complexity within the vertebrate *pard6* gene family that need to be further explored.

Materials and methods

Animals

Adult fish and embryos were maintained as described (Westerfield, 1995). We used wildtype and the following transgenic and mutant lines: *heart and soul*^{m567}, *nagie oko*^{m520}, *Tg(gutGFP)*^{s854}. *pard6γb*^{s441} was identified in a large-scale mutagenesis screen (Ober et al., 2006) .

Genotyping and cloning of four zebrafish pard6 genes

Genotyping of *pard6γb*^{s441} and *nok/mpp5*^{m520} embryos was performed using PCR and restriction fragment length polymorphisms or a dCAPS (Neff et al., 2002). Genotyping of *has/prkci*^{m567} was performed as previously described (Horne-Badovinac et al., 2001). We amplified full-length cDNA clones of *pard6γb* (accession NM 212563) and *pard6γa* (accession XM 689469) using PCR. Based on available human and mouse protein sequences, zebrafish genomic sequences, predicted sequences, published EST clones, and 5′-RACE analysis, we amplified full-length cDNA clones for *pard6α* (accession EF550990) and *pard6β* (accession EF550991), and introduced them into pCS2^{+}. Deletion constructs were generated by PCR as described in Bit-Avragim et al. (2008b). All constructs were sequenced for accuracy. All primer sequences are available upon request.

Fusion proteins

To generate fusion proteins, eGFP or mCherry (Shu et al., 2006) followed by a short amino acid sequence (S-G-G-G-G-S) were placed into the existing expression constructs at the 5′ end of the coding sequence creating fluorescent N-terminal fusion proteins.

In situ hybridization

We designed *in situ* probes that targeted the 3′end and included portions of the 3′-UTR of the zebrafish *pard6* genes. These sequences were cloned into pCRII (Invitrogen) and antisense DIG-labeled RNA probes were made using the appropriate SP6 or T7 promoters. We also utilized an existing *myl7* (formerly *cmlc2*) probe (Yelon et al., 1999). Whole mount *in situ* hybridization was performed as described (Alexander et al., 1998).

Morpholino and mRNA injections

For morpholino injections, 2ng of a splice-blocking morpholino designed against *pard6γb* (5′-ACATTCAACTCACCTTGCTTTTCAC-3′), a splice-blocking morpholino designed against *pard6α* (5′-TATTTAATG-TAGGGACTCACCTCTC-3′), or a *pard3* ATG morpholino (Wei et al., 2004) was injected into the yolk of wildtype embryos. For mRNA injections, we used the different constructs synthesized for the zebrafish Pard6 family: *pard6γa*, *pard6γb*, *pard6α*, *pard6β*, *pard6γa-gfp*, *pard6γb-mch*, *pard6α-gfp*, *pard6β-gfp*, *pard6γb(Δcrib)*, *pard6γb (Δpb1)*, *pard6γb(Δcrib)-gfp*, and *pard6γb(Δpb1)-gfp*. The generation of the mutant *pard6γb* constructs was described in Bit-Avragim et al. (2008b). Two additional constructs were kindly provided by other laboratories, *pard3-gfp* (Geldmacher-Voss et al., 2003), and *h2b-mrfp* (Megason and Fraser, 2003). Capped RNA was synthesized *in vitro* by transcription with SP6 polymerase from the constructs described above using the mMessage SP6 kit (Ambion). mRNAs were injected in 2.3 nL aliquots (100–400 pg) into the yolk of zygotes of either wildtype or *pard6γb*^{s441} heterozygous incrosses. Several mRNA concentrations were tried for each rescue construct and only embryos showing clear fluorescent protein expression were analyzed.

Immunohistochemistry

Embryos were fixed in 4% PFA for 2 h at room temperature, mounted in 4% agarose, and sectioned to 200 μm using a vibratome. Sections were blocked in PBS with 4% BSA and 0.3% Triton for 1 h and treated with primary antibody overnight at 4 °C as applicable. We used the following primary antibodies: rabbit anti-aPKC (C-20) (Santa Cruz Biotechnology, 1:1000), rabbit anti-Nok/Mpp5 (Wei and Malicki, 2002), mouse anti-ZO-1 (Zymed, 1:200), mouse anti-β-catenin (BD Biosciences, 1:200), mouse anti γ-tubulin (Sigma, 1:200). Sections were washed and treated with Alexa Fluor conjugated secondary antibodies, Alexa Fluor conjugated phalloidin, or TO-PRO3 (Invitrogen) for 2 h at room temperature. Following washing, sections were mounted on slides in Vectashield and imaged on a Zeiss LSM Pascal confocal microscope. Images were further analyzed using Image J Software including application of median filters.

Live imaging

To image the brain ventricles, embryos were prepared as previously described (Lowery and Sive, 2005). For imaging fusion proteins and time series, embryos were treated with Tricaine and mounted in 1% agarose. Embryos were analyzed on a Zeiss LSM5 Pascal confocal microscope or selective plane illumination microscopy (SPIM) set up (Huisken et al., 2004) and analyzed using Image J software.

Results

Identification and phenotypic analysis of s441

The *s441* mutant was identified in a forward genetic screen following ENU-induced mutagenesis (Ober et al., 2006). Compared to wildtype embryos at 36 hpf (Fig. 1A), *s441* mutants show phenotypes

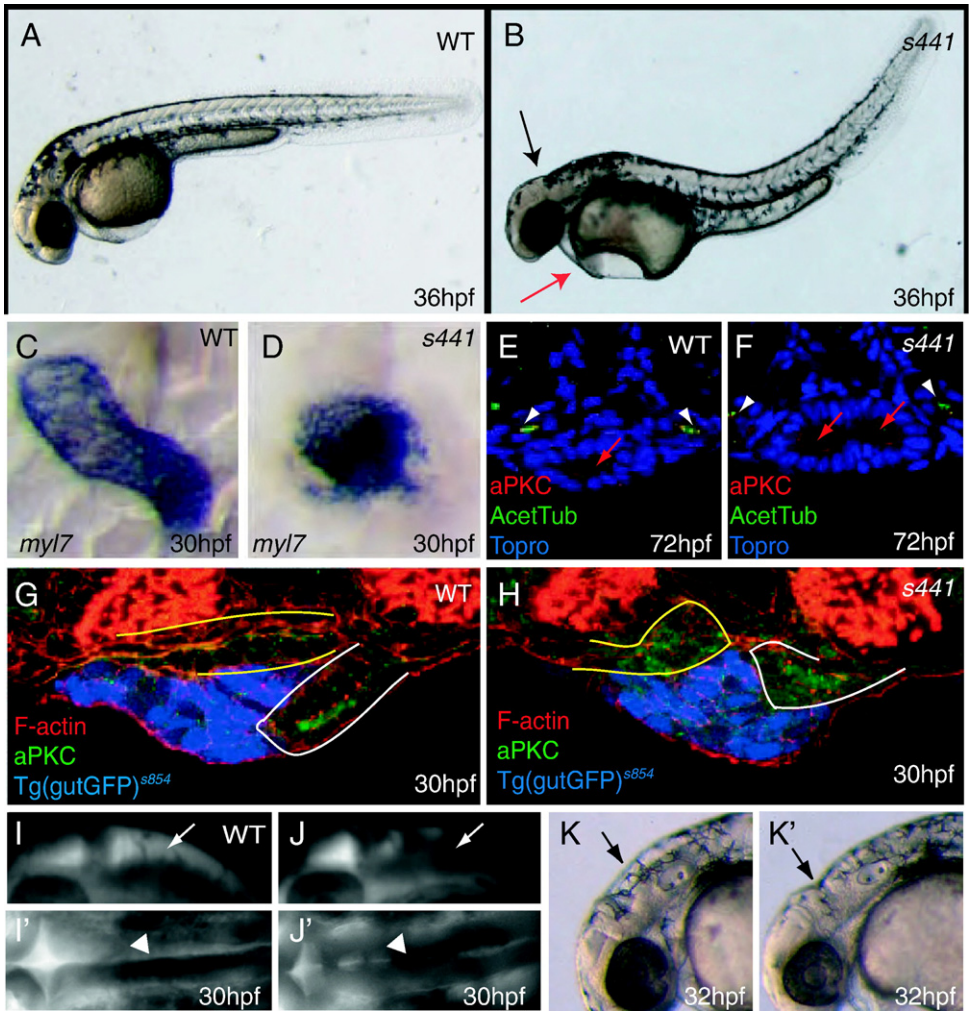

Fig. 1. *s441* mutants show defects in the development of organs derived from epithelial tissues. (A, B) Comparison of 36 hpf wildtype and *s441* mutant embryos. (B) *s441* mutant embryos show defects in heart development (red arrow), failure of the brain ventricles to inflate (black arrow), and dorsal curvature. (C, D) Dorsal views comparing 30 hpf wildtype and *s441* mutant hearts as assessed by *myl7* expression. (C) In wildtype embryos, the heart elongates to form a tube. (D) In *s441* mutant embryos, the heart fails to elongate. (E, F) Transverse sections of 72 hpf wildtype and *s441* mutant larvae through a region just posterior to the endodermal organ-forming region. The pronephric ducts marked by acetylated-tubulin staining are also visible in these sections (white arrowheads). (E) Wildtype larvae form one polarized lumen in the posterior gut (red arrow). (F) *s441* mutants occasionally show multiple lumens in the gut (red arrows). (G, H) Transverse sections of 30 hpf *Tg(gutGFP)*^{s854} wildtype and *s441* mutant embryos. Sections are through the endodermal organ-forming region and were stained for filamentous actin and aPKC. (G) In wildtype embryos, the right side of the LPM (outlined in white) moves ventrally towards the endoderm while the left side (outlined in yellow) moves dorsally. (H) In *s441* mutant embryos, the LPM fails to undergo asymmetric morphogenesis and both sides move dorsal to the endoderm. (I, J) Rhodamine dextran injected ventricles. Lateral (I) and dorsal (I') views show that wildtype embryos have well-inflated (arrow) and continuous (arrowhead) brain ventricles. Lateral (J) and dorsal (J') views illustrate that *s441* mutant embryos do not form fully inflated brain ventricles (arrow) and that the lumen is discontinuous (arrowhead). (K, K') Lateral views of 32 hpf wildtype and *s441* mutant embryos show the absence of an inflated hindbrain ventricle (arrows) in mutants compared to wildtype.

similar to the apicobasal polarity mutants *has/prkci* (Horne-Badovinac et al., 2001; Peterson et al., 2001), *nok/mpp5* (Wei and Malicki, 2002), *ome/crb2* (Omori and Malicki, 2006), and *moe/epb41l5* (Jensen and Westerfield, 2004) including pericardial edema, failure of the brain ventricles to inflate, and dorsal body curvature (Fig. 1B). Complementation analyses showed that *s441* was different from these four apicobasal polarity mutants (data not shown).

Since *s441* mutants share several phenotypes with mutants known to have defects in epithelial tissues, we investigated epithelial tissues and their derivatives in *s441* mutants. We examined the morphology of the myocardium (Figs. 1C–D), gut lumen formation (Figs. 1E–F), epithelial integrity and asymmetric migration of the lateral plate mesoderm (LPM) (Figs. 1G–H), and brain ventricle inflation (Figs. 1I–K'). We found developmental defects in all of these tissues in *s441* mutants. Thus, the *s441* mutation causes phenotypes indicative of apicobasal polarity defects and affects the development of organs derived from epithelial tissues.

s441 mutants show multiple lumens in the neural tube

While investigating the brain ventricles of *s441* mutants, we observed a novel phenotype (Belting and Affolter, 2007). Prior to 24 hpf in wildtype embryos, two continuous apical membranes form along the midline to surround a lumen, the neurocoel, which extends from the anterior brain ventricles to the posterior neural tube (Geldmacher-Voss et al., 2003). In wildtype embryos, F-actin (Fig. 2A), β-catenin (Fig. 2C), aPKC/Prkci (Fig. 2E), Pard3-GFP (Fig. 2G), Nok/Mpp5 (Fig. 2I), and ZO-1 (Fig. 2K), all localize to these continuous apical membranes. In contrast, *s441* mutant neural tubes lack continuous apical membranes. In regions where apical markers are present, small lumens form, while in regions where no apical markers are present, no lumens form (Figs. 2B, D, F, H, J, L). This 'mosaicism' is present along both the dorso-ventral (Fig. 2) and antero-posterior axes (see Fig. 6). In wildtype embryos, the nuclei align away from the midline and thus toward the basolateral membranes (Fig. 2M). In unpolarized regions of *s441* mutant neural tubes, the nuclei appear disorganized (Fig. 2N). Often, nuclei lie directly across the midline. Because *s441* mutant neural tubes also show discontinuous apical membranes at 48 (Figs. 2O–P) and 72 hpf (data not shown), this phenotype, which is fully penetrant (n>400 mutants examined), does not appear to be a consequence of developmental delay. These observations suggest that the *s441* mutation alters the function of a protein involved in neurocoel morphogenesis.

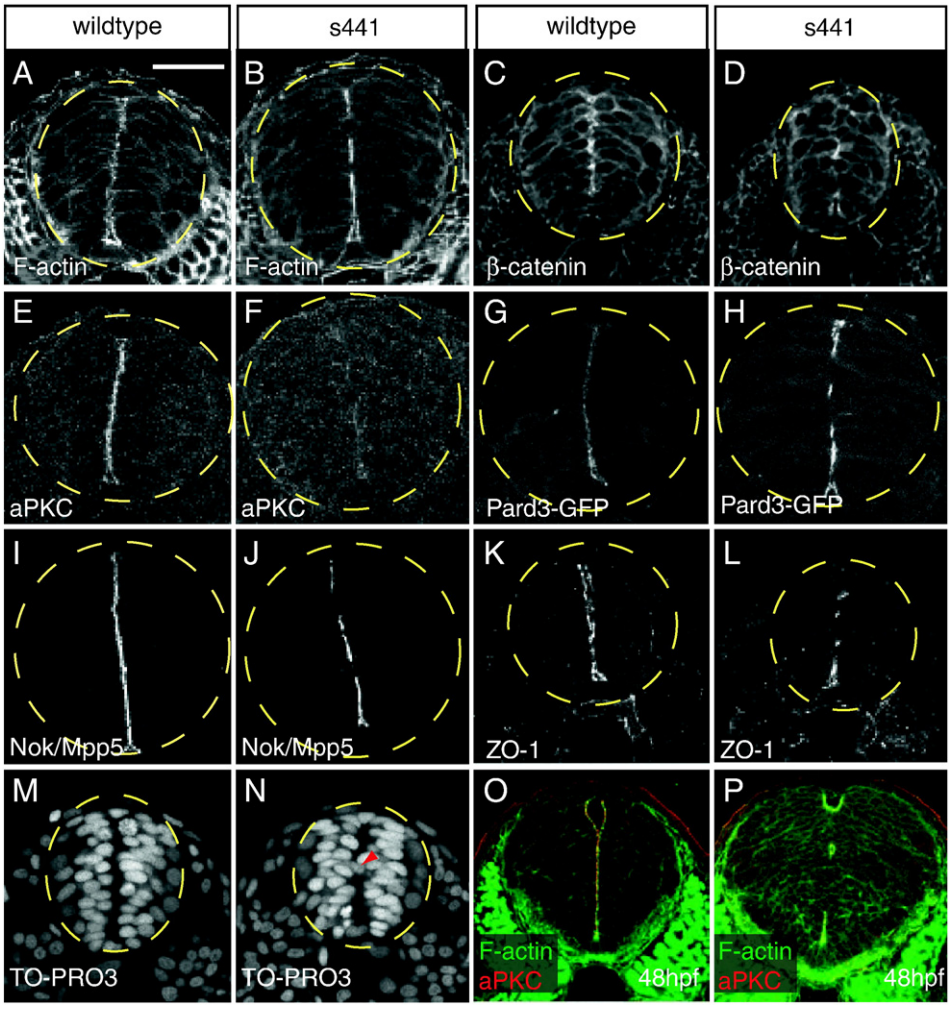

Fig. 2. *s441* mutants fail to form continuous apical membranes in the neural tube. (A-P) Transverse sections through wildtype and *s441* mutant neural tubes between the first and eighth somite at 24 (A–N) and 48 hpf (O–P). The dashed yellow circles outline the neural tube. Embryos were analyzed for localization of filamentous actin (A, B), β-catenin (C, D), aPKC (E, F), Pard3:GFP (G, H), Nok/Mpp5 (I–J), ZO-1 (K, L), TO-PRO3 (M, N), and both filamentous actin and aPKC (O–P). (A, C, E, G, I, K) Wildtype embryos form continuous apical membranes. (B, D, F, H, J, L) *s441* mutant embryos form discontinuous apical membranes. (F) Note that apical aPKC levels are dramatically reduced in *s441* mutants. (M) In wildtype neural tubes, nuclei are organized and positioned away from the midline. (N) In *s441* mutant neural tubes, some nuclei (arrowhead) are positioned across the midline. (panels O–P) At 48 hpf, the apical membranes in the *s441* mutant neural tubes remain discontinuous. Scale bar represents 50 μm and is applicable to all panels in this figure.

Positional cloning of pard6γb^{s441}

To get a better understanding of the *s441* phenotypes, we utilized a positional cloning approach to isolate the affected gene. The *s441* lesion was initially mapped to Chromosome 19 using bulk segregant analysis (Johnson et al., 1996). Fine mapping with 720 diploid embryos localized the *s441* lesion to a region flanked by the simple sequence length polymorphisms (SSLP) markers z6079 and z9059. This region was narrowed using newly designed SSLP markers targeting CA-repeats (Fig. 3A). Examination of the genomic region between the two closest markers revealed the existence of three ESTs, one of which being *pard6γb* (Fig. 3A). Because *pard6* genes are known to play a role in apicobasal polarity in multiple organisms (Watts et al., 1996; Joberty et al., 2000; Lin et al., 2000; Petronczki and Knoblich, 2001), we tested *pard6γb* as a candidate for the gene affected by the *s441* mutation.

To test whether a mutation in *pard6γb* caused the *s441* phenotype, we took several approaches including analyzing the *pard6γb* expression pattern. *pard6γb* mRNA is maternally deposited (Fig. 3B). At 10 hpf, its expression is ubiquitous and extends along the axial region of the embryo (Fig. 3C). Later at 18 (Fig. 3D) and 24 hpf (Fig. 3E), *pard6γb* maintains its ubiquitous expression but becomes heightened in regions of the embryo that form epithelial structures. This heightened expression is particularly noticeable in regions of the neural tube (Figs. 1C–E; ZFIN, Thisse et al., 2001). This expression pattern is consistent with the tissues affected in *s441* mutants. Second, we compared cDNA sequences of the wildtype and *s441* mutant alleles of *pard6γb*. The 1302 base pairs of wildtype sequence encode a 434 amino acid protein. The mutant allele showed a base change from T to A at position 192 creating a premature stop codon at amino acid 64 (Figs. 3F–H). This single base change was confirmed by comparing genomic DNA sequences of the wildtype and *s441* mutant alleles of *pard6γb*. To complement the information gained through genetic mapping, we injected morpholino antisense oligonucleotides designed against *pard6γb* to test whether lack of wildtype Pard6γb was responsible for the *s441* mutant phenotypes. Injection of 2 ng of a morpholino that blocks splicing between the first and second exon of the *pard6γb* transcript (Fig. 3A) phenocopied the *s441* mutant in 92% of the injected embryos (n=98/106) (Fig. 3I). Morpholino-injected embryos showed defects in heart morphogenesis, failure of the brain ventricles to inflate, dorsal body curvature (Fig. 3I), and a discontinuous neurocoel (data not shown). To further test the hypothesis that the *s441* mutation affects *pard6γb*, we injected 200 pg of full-length, wildtype *pard6γb* mRNA into embryos from heterozygous incrosses.

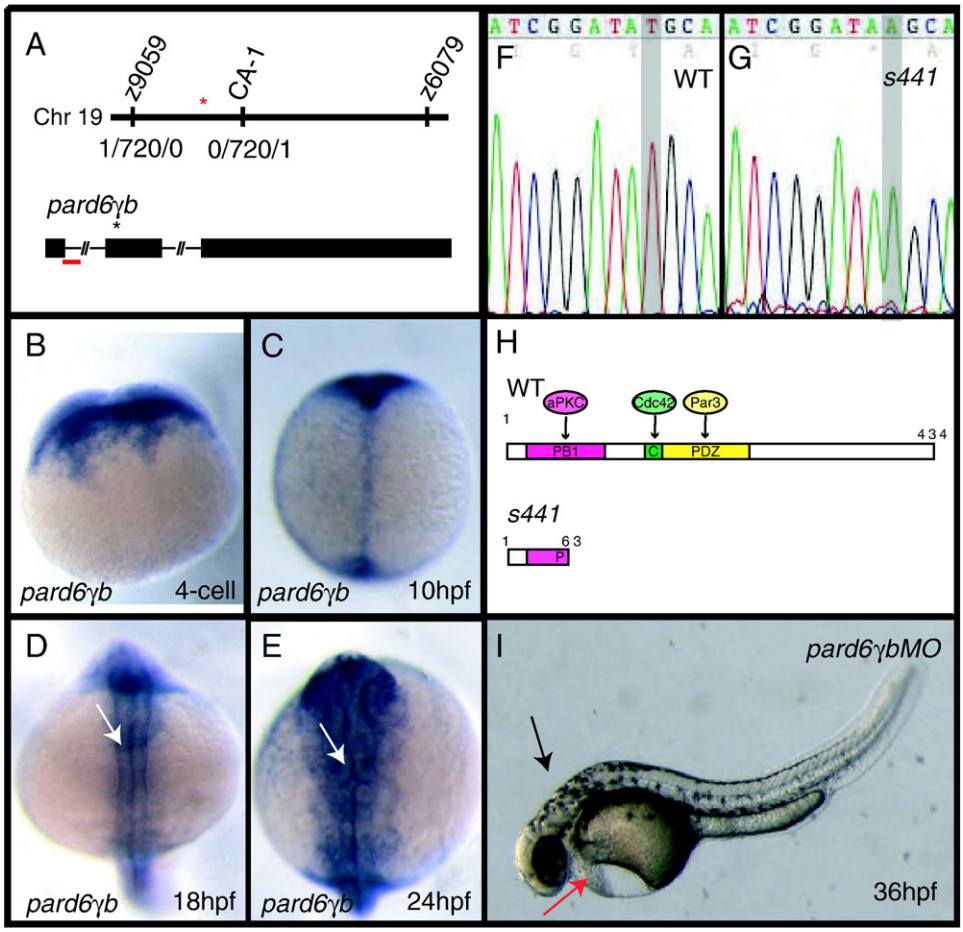

Fig. 3. *s441* is a mutation in *pard6γb*. (A) Positional cloning of *s441*. *s441* was linked to a region on Chromosome 19 between the SSLP markers z9059 and z6079. Using an additional SSLP marker (labeled CA-1) the position of the mutation was narrowed to a region flanked by two recombinants, each unique to one side. The red asterisk represents the location of *pard6γb*. *pard6γb* contains three exons (rectangles) and two introns (lines). The black asterisk represents the lesion. The red bar represents the region targeted by the splice-blocking morpholino. (B–E) Expression of *pard6γb*. (B) *pard6γb* mRNA is maternally deposited. (C) At 10 hpf, *pard6γb* appears to be expressed ubiquitously. (D, E) At 18 and 24 hpf, *pard6γb* appears to be expressed in all tissues and shows heightened expression in the neural tube (arrows). (F, G) Sequence analysis of wildtype versus *s441 pard6γb* cDNA revealed a T to A (gray highlight in panels H and I) transition 192 base pairs following the start of translation. (H) Schematic of the PB1, CRIB (abbreviated C), and PDZ domains and the predicted protein-protein interactions with the wildtype protein. The premature stop codon caused by the *s441* mutation leads to a protein truncated at amino acid 63. Numbers shown represent amino acid position. (I) Injecting 2 ng of a splice morpholino designed against the first exon-intron boundary phenocopied the *s441* mutation. The morphants showed defects in heart development (red arrow), failure of the brain ventricles to inflate (black arrow), and dorsal curvature.

Injection of this mRNA resulted in 97% (n=114/117) of the offspring displaying no phenotype at 30 hpf. In addition, injection of *s441* mutant *pard6γb* mRNA into *s441* heterozygous incrosses resulted in 23% (n=65/282) of the offspring displaying the mutant phenotype, similar to uninjected incrosses. In similar injection experiments where embryos from heterozygous incrosses were injected with wildtype *pard6γb* mRNA and genotyped, 22 of 25 mutants were rescued. There was no observed phenotype caused by overexpression of Pard6γb at the quantities required for rescue. Altogether, the results from the genetic mapping, expression, allele sequence, morpholino, and mRNA rescue analyses indicate that the *s441* mutation is caused by a lesion in *pard6γb*. Therefore, *s441* will be referred to as *pard6γb*^{s441}.

Localization of Pard6γb protein during neurulation

To determine the subcellular localization of Pard6γb, we constructed N-terminal fusion proteins between mCherry and Pard6γb (Pard6γb-mCh), as well as GFP and Pard6γb (Pard6γb-GFP). The addition of a fluorescent tag did not disrupt the function of these fusion proteins as evidenced by the ability of injected *pard6γb-mch* and *pard6γb-gfp* mRNA to rescue the *pard6γb*^{s441} phenotypes. Both fusion proteins showed a stage-dependent pattern of localization. In contrast to the cytoplasmic localization of Pard3-GFP at 10 hpf (Fig. S1A), the Pard6γb fusion proteins localized primarily to the nucleus (Figs. S1B–C). Following gastrulation, Pard6γb fusion proteins continued to localize to the nucleus and some protein also localized to the cytoplasm and cell membranes (Fig. S1D). During the neural keel stage, when cells divide across the midline (termed mirror symmetric cell divisions) and Pard3-GFP localizes to the cleavage furrow of cells during cytokinesis (Tawk et al., 2007), Pard6γb-GFP shows an analogous localization (Figs. S2A–C). After the neural keel stage, Pard6γb-mCh began to localize to the midline of the neural tube (Figs. 4A–B). As the apical membranes of the neurocoel formed and became continuous, both Pard6γb-mCh and Pard3-GFP became primarily localized to this surface (Figs. 4C–D). Through our analyses, however, we could not discern whether Pard3-GFP or Pard6γb-mCh localized to the apical membranes prior to the other one. Similar to the localization pattern of Pard3-GFP (Geldmacher-Voss et al., 2003), a low amount of Pard6γb-mCh remained in the cytoplasm. Thus, in contrast to Pard3-GFP localization prior to gastrulation, Pard6γb-mCherry and Pard6γb-GFP localize primarily to the nucleus, and during the neural keel, rod, and tube stages, they localize to the apical membranes of the neural tube and behave like Pard3-GFP.

Lack of Pard6γb function alters late mitotic behaviors in the embryonic neural tube

Previous research has shown that the placement of Pard3-GFP during mirror symmetric cell divisions at the neural keel stage is

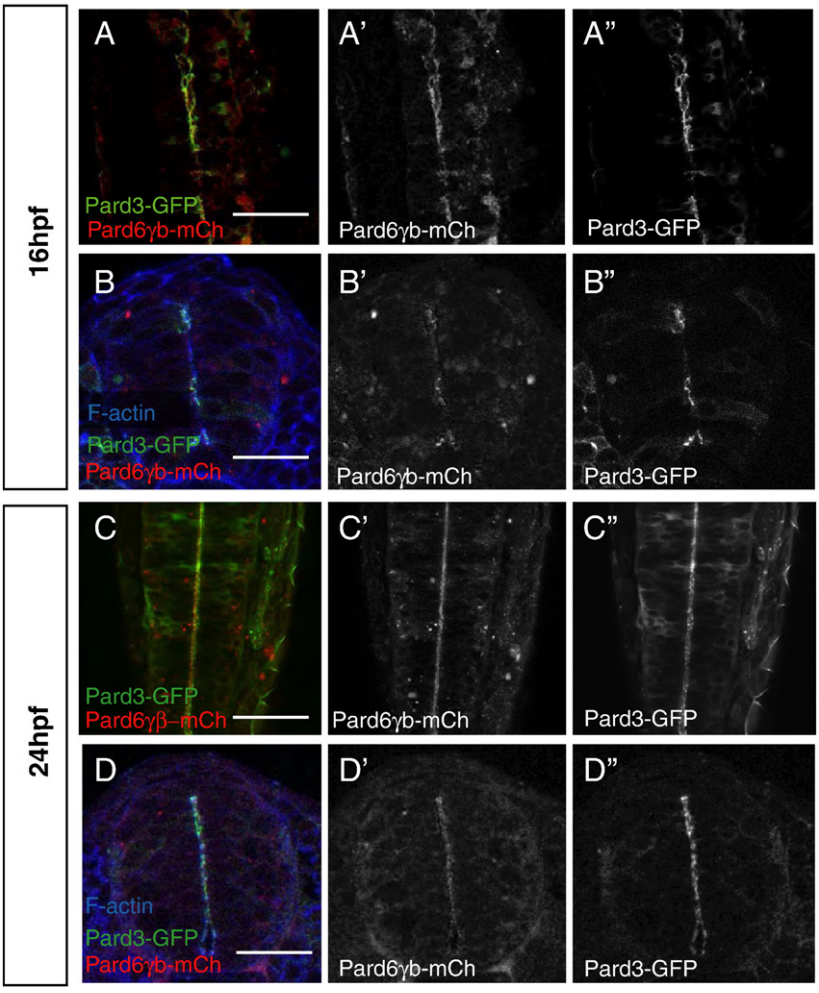

Fig. 4. Distribution of Pard6γb during neurulation. (A–D) All embryos were injected with *pard3-gfp* and *pard6γb-mch* mRNA. (A, C) Optical sections through the neural tube of live embryos (dorsal views between the first and sixth somite, anterior up). (B, D) Transverse sections through the neural tube of embryos between the first and sixth somite stained for filamentous actin. (A, B) At 16 hpf, Pard6γb-mCh begins to localize with Pard3-GFP to the forming apical membranes of the neural tube. (C, D) At 24 hpf, Pard6γb-mCh localizes with Pard3-GFP along the maturing apical membranes of the neural tube. Scale bars represent 50 μm.

important for the location of the future neurocoel (Tawk et al., 2007). At later stages, there is evidence that the re-orientation of cell division in the neural tube of zebrafish embryos is dependent on the function of the Pard3/Pard6/Prkci complex (Geldmacher-Voss et al., 2003). The multiple lumen phenotype in *pard6γb*^{s441} mutants prompted us to re-examine the role of apicobasal polarity and specifically the function of the Pard3/Pard6/Prkci complex in orienting mitoses at the neural keel and neural tube stages.

First, we examined *pard6γb* morphants prior to 18 hpf, when mitoses occur in an orientation perpendicular to the midline and daughter cells end up on opposite sides of the midline (Geldmacher-Voss et al., 2003; Ciruna et al., 2006; Tawk et al., 2007). We also injected these embryos with *pard3-gfp* and *ras-mcherry* mRNA to facilitate this analysis, and observed no difference in cell behavior, or Pard3-GPF localization, compared to control (n=12 morphants; data not shown). Cells underwent mirror symmetric cell divisions and Pard3-GFP localized to the cleavage furrow of dividing cells.

Second, we examined embryos after 21 hpf, when, in wildtype, the apical membranes along the neurocoel have become continuous and the orientation of mitoses has changed by 90° (Geldmacher-Voss et al.,

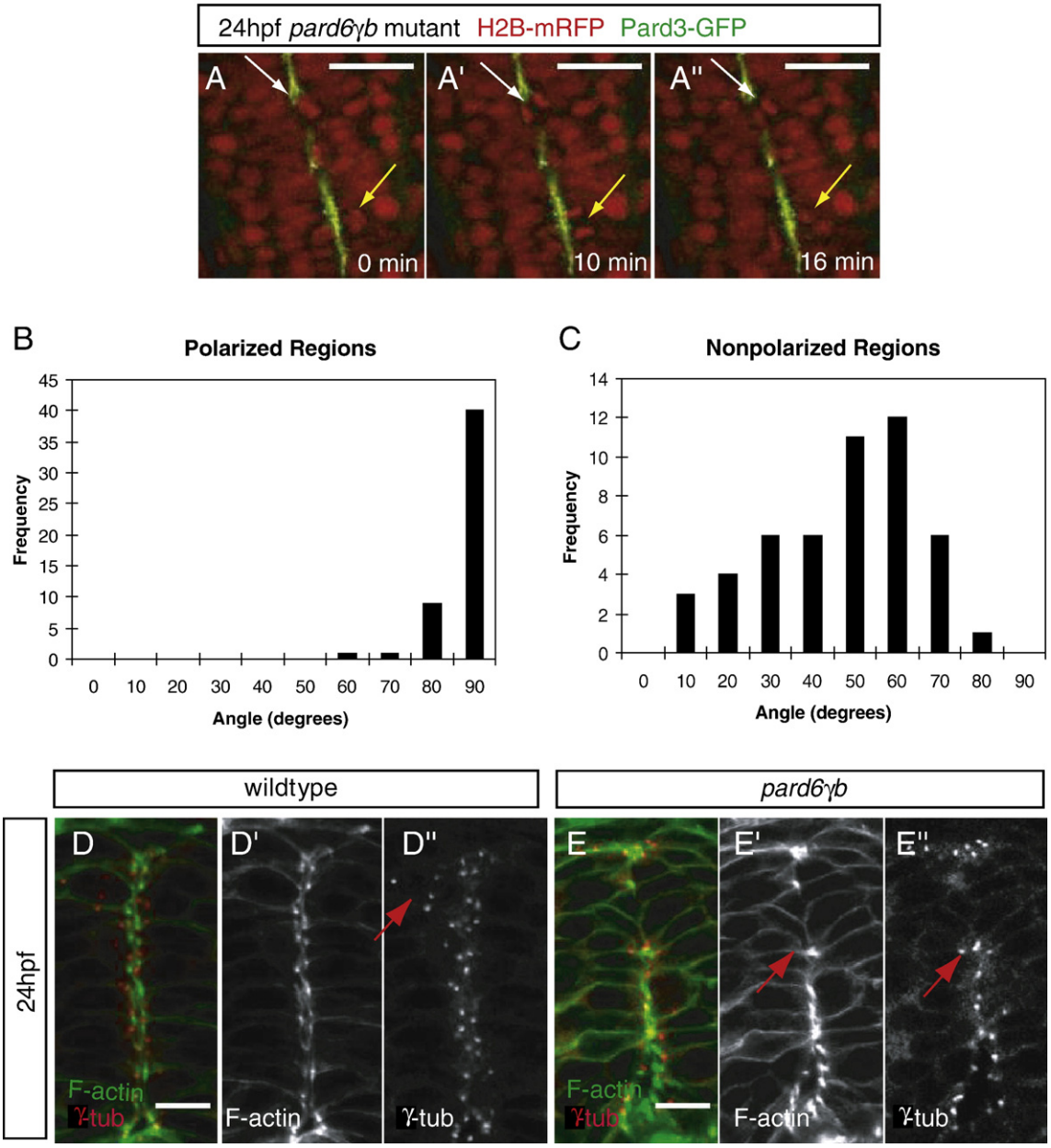

Fig. 5. Position of the apical membranes in the neural tube appears to regulate the orientation of mitoses and the positioning of centrosomes during the neural tube stage. (A) Time lapse images of a 24 hpf *pard6γb*^{s441} mutant embryo injected with *pard3-gfp* and *h2b-mrfp* mRNA (dorsal views between the first and sixth somite, anterior to the top). Time is indicated in minutes. The yellow arrow points to a cell division in a region of continuous polarity, at an 88° angle (see B). The white arrow points to a cell division in a region of discontinuous polarity, at a 26° angle (see panel C). (B, C) Schematic of the technique used to analyze the angle of cell division in wildtype and *pard6γb*^{s441} mutant embryos. The angle between the midline (green) of the neural tube and the cleavage plane (black) of two dividing nuclei was recorded and analyzed on a histogram using the value ≤90°. (B) In regions with polarized localization of Pard3-GFP in wildtype (n=3) and *pard6γb*^{s441} mutant (n=12) embryos, the angle of division clustered between 80° and 90° (n=40/50). (C) In regions lacking polarized localization of Pard3-GFP in *pard6γb*^{s441} mutant embryos, the angle of division clustered between 40° and 70° (n=29/50). (D, E) Transverse sections through the neural tube between the first and sixth somite of 24 hpf embryos, stained for filamentous actin and γ-Tubulin. (D) In wildtype embryos, centrosomes are localized along the apical side of the cells lining the neurocoel or rotated 90° when cells are dividing (arrow). (panel F) In *pard6γb*^{s441} mutant embryos, centrosomes are positioned as in wildtype when polarized apical membranes are present, but appear to be missing or mislocalized in nonpolarized regions. The arrow points to a cell that has re-oriented the position of its centrosome towards a polarized region. Scale bars in panel A represent 50 μm, and in panels D and E 10 μm.

2003). We analyzed mitotic events between 22–25 hpf in the neural tube of live wildtype and *pard6γb*^{s441} mutants that had been injected with *pard3-gfp* and *h2b-mrfp* mRNA. We examined mitoses in regions where Pard3-GFP localized continuously along the midline in wildtype and *pard6γb*^{s441} mutant embryos (Figs. 5A–E) as well as mitoses in regions lacking Pard3-GFP localization in *pard6γb*^{s441} mutants (Figs. 5A and C). [We only analyzed mitotic events where we could clearly measure the angle of division and daughter cells remained in close proximity to their mother cell.] By measuring the angle of the plane of division in reference to the midline of the neural tube, we found that in polarized regions in both wildtype and mutant embryos, the angle of mitoses was tightly clustered between 80° and 90° (n=40/50 cell divisions) (Fig. 5B), in agreement with previous reports (Geldmacher-Voss et al., 2003; Reugels et al., 2006; von Trotha et al., 2006). In regions lacking polarity, we found the angle of mitoses to cluster between 40° and 70° (n=29/50 cell divisions) (Fig. 5C), a more dramatic effect than that observed in other polarity mutants or morphants (Geldmacher-Voss et al., 2003). Looking at this phenotype in more detail, we observed that in unpolarized regions that were 1-3 cells long, cells appeared to use information from nearby or surrounding polarized regions to orient mitotic divisions. In the rare situations when cell divisions occurred in larger unpolarized regions, the orientation of division was similar to that of cells prior to 18 hpf. These data show that the multiple lumen phenotype of *pard6γb*^{s441} mutants correlates with altered cell behavior at the neural tube stage.

Functional analysis of Pard6γb protein-protein interaction domains during neurocoel formation

Experiments in *C. elegans* (Gotta et al., 2001), *Drosophila* (Hutterer et al., 2004), and MDCK cells (Joberty et al., 2000; Lin et al., 2000; Qiu et al., 2000; Hurd et al., 2003) have provided evidence that Pard6 function is dependent on three main protein-protein interaction domains: the PB1, CRIB, and PDZ domains. The PB1 domain interacts with Prkci, the CRIB domain interacts with Cdc42, and the PDZ domain (specifically the KPLG sequence) interacts with both Pals1 (Nok/Mpp5) and Pard3. These data prompted us to ask whether a particular domain of the Pard6γb protein was required for Pard6γb function in forming a continuous neurocoel.

In order to examine specifically how the PB1 and CRIB domains as well as the PDZ domain, which contains a KPLG motif essential for protein binding, affect Pard6γb localization and function, we constructed deletion alleles that eliminated the PB1 (ΔPB1) or CRIB (ΔCRIB) domain, and altered the KPLG amino acid sequence to AAAA. Injection of *pard6γb(Δpb1)*, *pard6γb(Δcrib)*, or *pard6γb(kplg)* mRNA did not rescue any of the *pard6γb*^{s441} phenotypes (data not shown). In

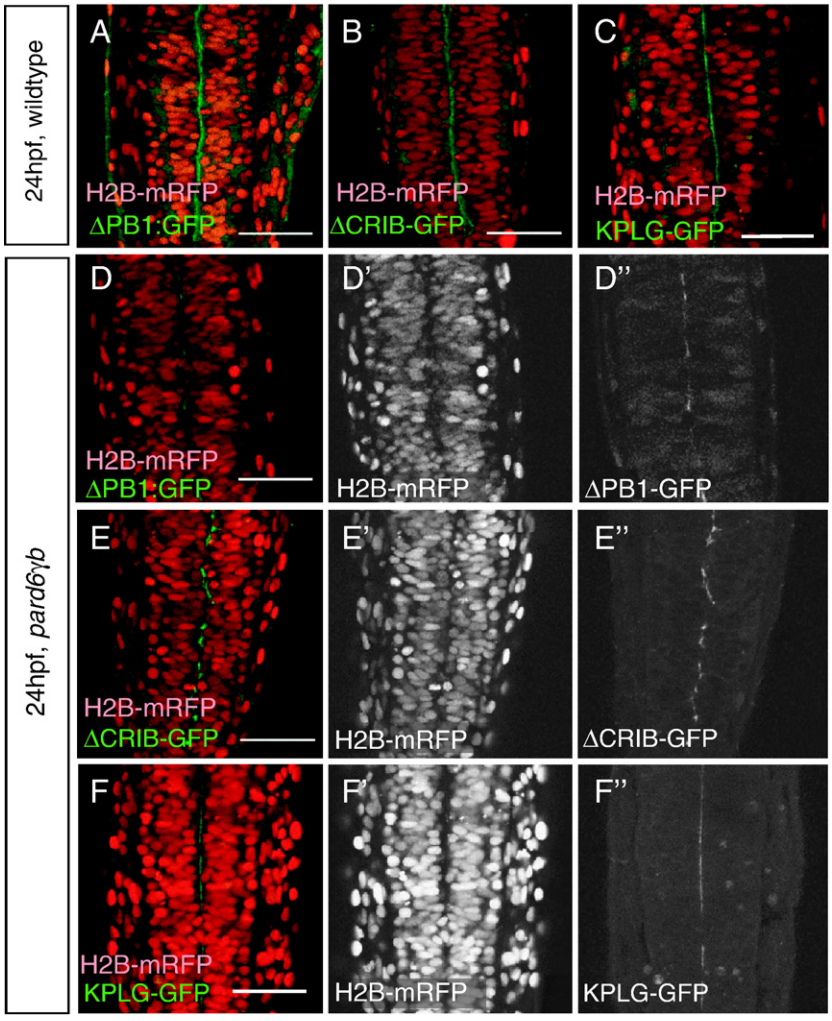

Fig. 6. The PB1, CRIB and PDZ domains are required for Pard6γb function but not localization. (A–E) Live, 24 hpf embryos injected with *h2b-mRFP* and *pard6γb(Δpb1)-GFP* (abbreviated ΔPB1-GFP), *pard6γb(Δcrib)-GFP* (abbreviated ΔCRIB-GFP) or *pard6γb*(kplg)*-GFP* (abbreviated KPLG-GFP) mRNA as indicated (dorsal views between the first and sixth somite, anterior to the top). (A–C) In wildtype neural tubes, nuclei are organized on either side of the midline. (D-F) In *pard6γb*^{s441} mutant neural tubes, nuclei are disorganized. In wildtype embryos, ΔPB1-GFP (A), ΔCRIB-GFP (B) and KPLG-GFP (C) localized to the cytoplasm and apical membranes. In *pard6γb*^{s441} mutant embryos, ΔPB1-GFP (D), ΔCRIB-GFP (E) and KPLG-GFP (F) failed to rescue the mutant phenotype and localized to the discontinuous apical membranes. Scale bars represent 50 μm.

order to analyze the localization of these proteins, we created fusion constructs and injected *h2b-mRFP* (a nuclear marker) and *pard6γb (Δpb1)-GFP, pard6γb(Δcrib)-GFP,* or *pard6γb(kplg)-GFP* mRNA into heterozygous *pard6γb*^{s441} incrosses and analyzed GFP localization in the neural tube of live embryos at 24 hpf. In 24 hpf wildtype embryos, Pard6γb(ΔPB1)-GFP localized primarily to the apical membranes around the neurocoel as well as the cytoplasm (Fig. 6A). In 24 hpf *pard6γb*^{s441} mutant embryos, Pard6γb(ΔPB1)-GFP localized primarily to the discontinuous apical membranes as well as the cytoplasm (Fig. 6D). In 24 hpf wildtype embryos, Pard6γb(ΔCRIB)-GFP localized to the cytoplasm as well as the apical membranes (Fig. 6B). In *pard6γb*^{s441} mutant embryos, Pard6γb(ΔCRIB)-GFP was found in the cytoplasm and the discontinuous apical membranes (Fig. 6E). Pard6γb (KPLG)-GFP exhibited similar localization as Pard6γb(ΔPB1)-GFP and Pard6γb(ΔCRIB)-GFP in wildtype (Fig. 6C) and *pard6γb*^{s441} mutants (Fig. 6F).

These data indicate that the PB1, CRIB and KPLG interaction domains are all required for Pard6γb function during neurocoel formation but not for Pard6γb localization *in vivo*. Alternatively, the presence of maternally derived Pard6γb or of other members of the Pard6 family may mask the requirement of these domains for Pard6γb localization.

In order to further analyze the role of the Par3/Par6/aPKC complex in apical membrane formation in the neural tube, we generated double mutants for *pard6γb* and *has/prkci*, *pard6γb* and *nok/mpp5*, as well as embryos with reduced levels of Pard6γb and Pard3. All three of

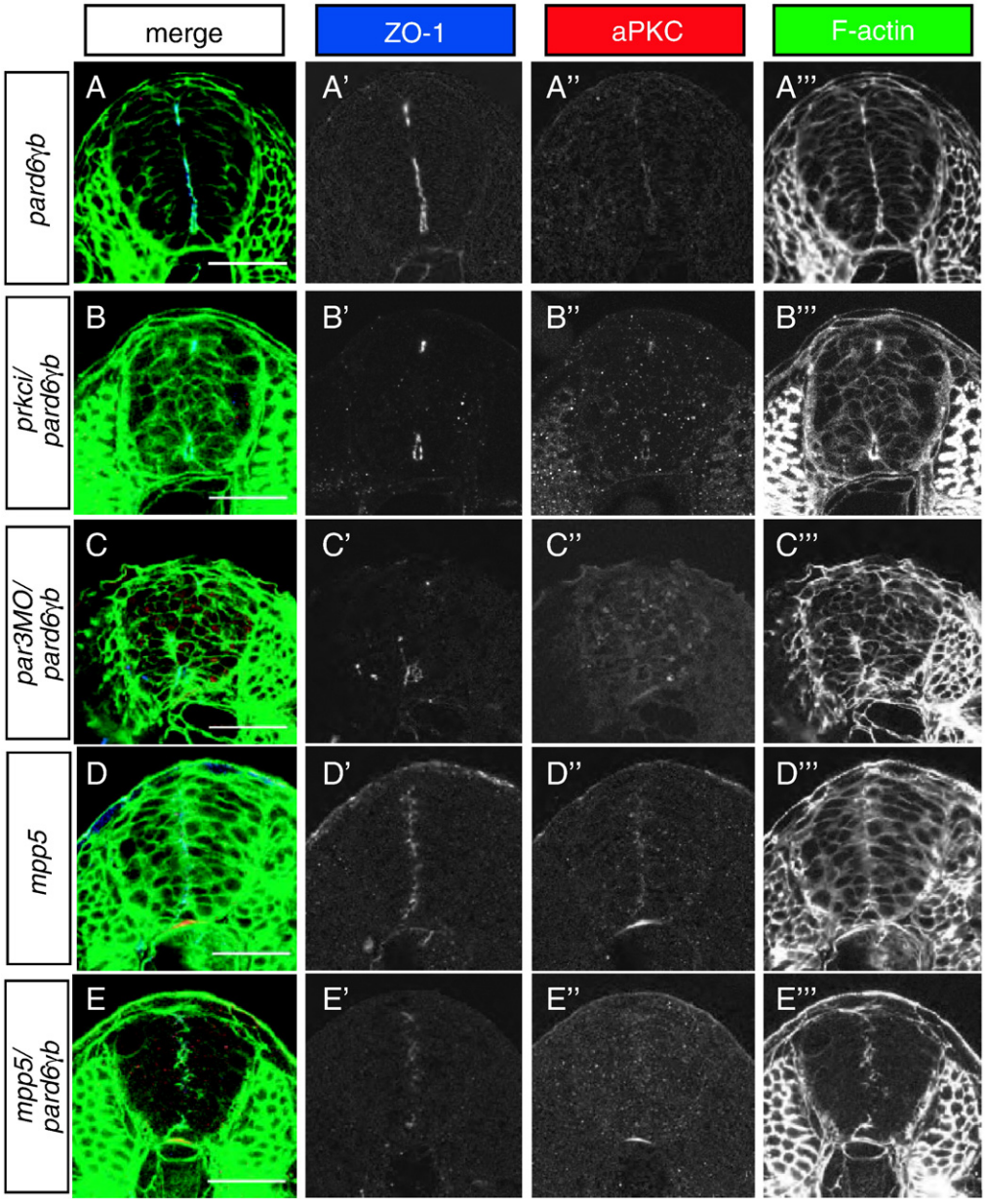

Fig. 7. Role of the Par3/Par6/aPKC complex in apical membrane formation in the neural tube. All images represent transverse sections between the first and sixth somite stained for ZO-1 (blue), aPKC (red), and filamentous actin (green) at 24 hpf. (A) *pard6γb*^{s441} mutant neural tubes show a reduced amount of apical membranes. (B) *pard6γb*^{s441}*/prkci* double mutants show a more severe reduction in apical membrane formation than *pard6γb*^{s441} mutants. (C) *pard6γb*^{s441} mutants injected with a *pard3* morpholino show a more severe reduction in apical membrane formation than *pard6γb*^{s441} mutants. (D) *mpp5* mutant neural tubes do not show an obvious severe reduction in apical membrane formation. (E) *pard6γb*^{s441}*/mpp5* double mutants show a more severe reduction in apical membrane formation than *pard6γb*^{s441} or *mpp5* single mutants. In addition, *pard6γb*^{s441}*/prkci* and *pard6γb*^{s441}*/mpp5* double mutants as well as *pard6γb*^{s441} mutants injected with a *pard3* morpholino exhibit a severe epithelial disorganization in the neural tube. Scale bars represent 50 μm.

these gene depletion strategies caused a more severe phenotype in apical membrane formation in the neural tube (Fig. 7). Apical membrane formation was much reduced in *pard6γb/prkci* double mutants (n=5) (Fig. 7B) compared to *pard6γb* (Fig. 7A) or *prkci* (data not shown) single mutants. Wildtype embryos injected with a *pard3* morpholino did not exhibit an obvious defect in apical membrane formation in the neural tube (data not shown), while embryos with reduced levels of Pard6γb and Pard3 (n=5) exhibited little apical

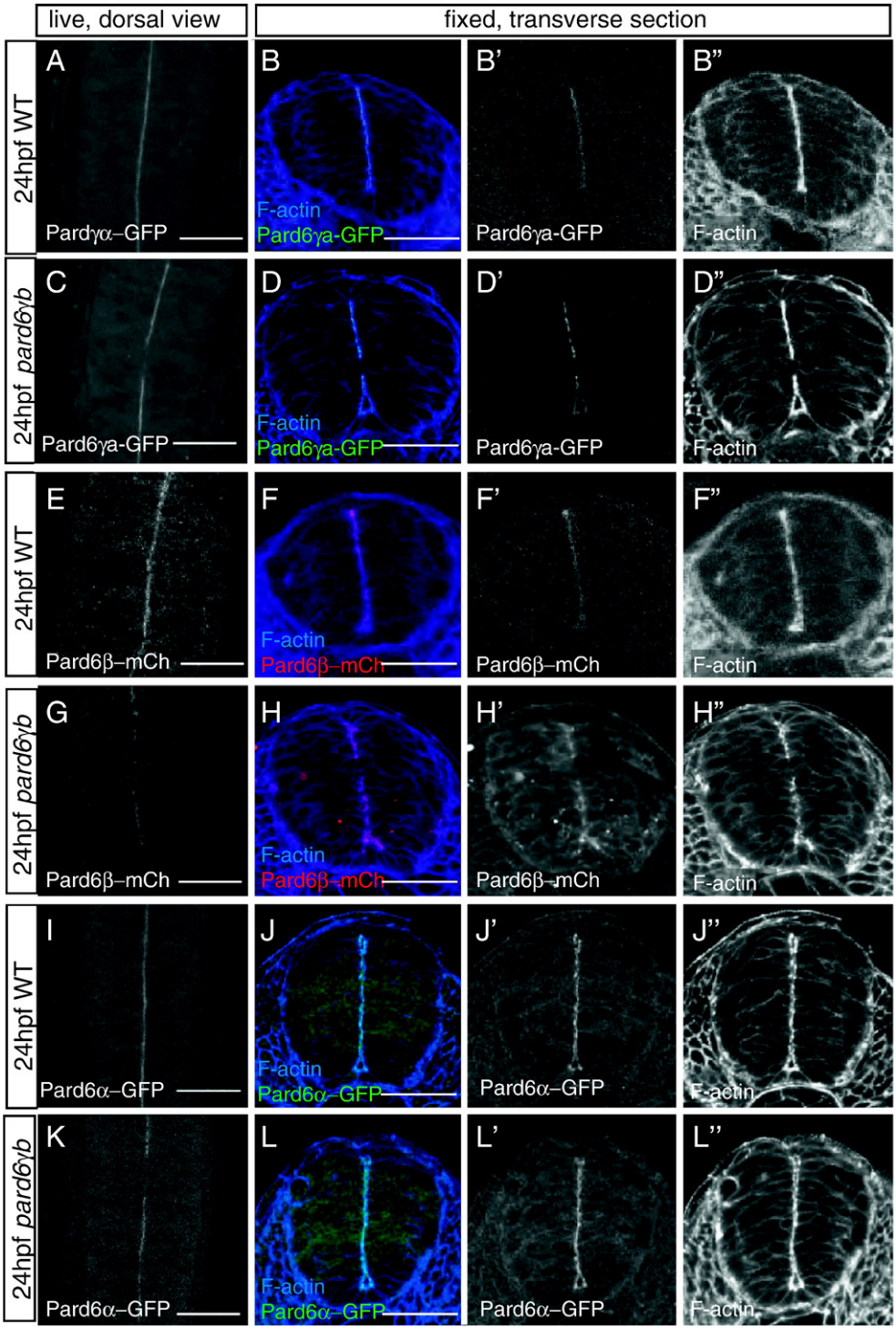

Fig. 8. Apical localization of the other Pard6 family members and partial rescue of the *pard6γb*^{s441} mutant phenotype by Pard6α. (A, C, E, G, I, K) Optical sections through the dorsal neural tube of live 24 hpf embryos between the first and sixth somite. (B, D, F, H, J, L) Transverse sections through the neural tube between the first and sixth somite of 24 hpf embryos, stained for filamentous actin. (A–D) Embryos injected with mRNA encoding Pard6γa-GFP. (A, B) In wildtype embryos, Pard6γa-GFP localized to the apical membranes. (panels C–D) In *pard6γb*^{s441} mutant embryos, Pard6γa-GFP localized to the discontinuous apical membranes, and it did not rescue the *s441* mutant phenotype. (E–H) Embryos injected with mRNA encoding Pard6β-mCh. (E, F) In wildtype embryos, Pard6β-mCh localized to the apical membranes. (G, H) in *pard6γb*^{s441} mutant embryos, Pard6β-mCh localized to the discontinuous apical membranes, and it did not rescue the *pard6γb*^{s441} mutant phenotype. (I–L) Embryos injected with mRNA encoding Pard6α-GFP. (I, J) In wildtype embryos, Pard6α-GFP localized to the apical membranes. (K, L) In *pard6γb*^{s441} mutant embryos, Pard6α-GFP localized to the apical membranes. (K) In this *pard6γb*^{s441} mutant embryo, midline Pard6α-GFP localization was discontinuous and Pard6α-GFP failed to rescue the neurocoel phenotype. (L) In another, and genotyped, *pard6γb*^{s441} mutant embryo, midline Pard6α-GFP localization was continuous and Pard6α-GFP rescued the neurocoel phenotype. Scale bars represent 50 μm.

membranes in their neural tube (Fig. 7C). In *nok/mpp5* single mutants, as previously reported by Lowery and Sive (2005), apical membranes in the neural tube may form in a continuous manner although the lumen does not inflate (Fig. 7D). In *pard6γb/mpp5* double mutants ($n=5$), apical membrane formation was much reduced (Fig. 7E). In addition, all three of these gene depletion strategies led to severe epithelial disorganization in the neural tube. Altogether these analyses indicate that these four proteins function redundantly to regulate apical membrane formation in the neural tube.

Analysis of maternal zygotic embryos

Since *pard6γb*^{s441} mutants can form some apical membranes in their neural tube, we tested two hypotheses: (1) the maternal contribution of Pard6γb provides sufficient function for some apical membranes to form, or (2) one or more of the additional Pard6 family members compensates for the loss of Pard6γb function in *pard6γb*^{s441} mutants.

In order to test the first hypothesis we examined the neural tube in *Maternal Zygotic (MZ) pard6γb*^{s441} mutants, which lack both the maternal and zygotic contribution of Pard6γb. Embryos from a *pard6γb*^{s441} heterozygous incross were injected with wildtype *pard6γb* mRNA and raised to adulthood. Several homozygous mutant adults were identified through genetic crosses and PCR genotyping. Crossing homozygous adults produced *MZpard6γb*^{s441} offspring. *MZpard6γb*^{s441} mutant embryos exhibit body phenotypes that are similar to, yet somewhat more severe than, zygotic mutants. In particular, the retinal pigmented epithelium of *MZpard6γb*^{s441} mutants showed a more severe phenotype than that of zygotic *pard6γb*^{s441} mutants (Fig. S3A), and more similar to *prkci* mutants. The severity of the neural tube phenotype in embryos lacking the maternal and zygotic component of *pard6γb* was similar to that of embryos that only lack the zygotic component (Fig. S3B), suggesting that the maternal contribution of Pard6γb does not explain the presence of apical membranes in zygotic *pard6γb*^{s441} mutants.

Identification and analysis of three additional Pard6 family members

To investigate the hypothesis that one or more of the additional Pard6 family members could compensate for the loss of Pard6γb function in *pard6γb*^{s441} mutants, we examined EST databases and genome browsers and found evidence for three additional *pard6* genes. We amplified full-length cDNA's for each of the additional *pard6* genes. All four zebrafish Pard6 proteins show high similarity to the *C. elegans* and mouse Pard6 proteins, especially in the PB1, CRIB, and PDZ domains (Fig. S4A). The gene names *pard6γa* (located on Chromosome 16) and *pard6γb* have already been assigned. Using information from the ClustalW analysis (Fig. S4B) and synteny considerations, the genes currently assigned to chromosomes 18 and 23 were named *pard6α* and *pard6β*, respectively.

We examined the expression patterns of each of the three additional *pard6* genes and found that they were all maternally deposited (data not shown), and subsequently showed similar expression patterns as *pard6γb*. There were, however, several distinct temporal and spatial expression patterns to note. For example, none of the other three *pard6* genes appeared to be expressed along the axial region at 10 hpf (data not shown) and pard6β showed heightened expression in the otic placodes beginning at 18 hpf and present at 24 hpf (Fig. S4C).

In order to determine whether any of the additional Pard6 family members could compensate for Pard6γb function, we constructed fluorescent fusion proteins (Pard6γa-GFP, Pard6β-mCh, and Pard6α-GFP) using the same method used for generating the functional Pard6γb-mCh. We injected 100-300 pg of mRNA encoding these fluorescent fusion proteins into heterozygous *pard6γb*^{s441} incrosses. Pard6γa-GFP (Figs. 8A–D) and Pard6β-mCh (Figs. 8E–H) localized to the apical membranes in the neural tube but did not rescue the *pard6γb*^{s441} mutant phenotype (Figs. 8C, D, G and H). Pard6α-GFP also localized to the apical membranes of the neural tube (Figs. 8I–L). When we examined Pard6α-GFP localization in *pard6γb*^{s441} heterozygous incrosses, we observed a lower percentage of affected embryos from these injected incrosses ($n=11/100$ embryos) compared to uninjected incrosses (24/100 embryos). In addition, some embryos showed wildtype-like brain ventricle inflation but maintained other *pard6γb*^{s441} mutant phenotypes including pericardial edema and body curvature (not shown).

To test whether the fluorescent tags were interfering with protein function, we also performed these same experiments by injecting untagged *pard6γa*, *pard6β*, and *pard6α* mRNA's into *pard6γb*^{s441} heterozygous incrosses. The results of these experiments were identical to the experiments with the fluorescent fusion proteins, indicating that the fluorescent tags were not disrupting protein function (data not shown). These data suggest that the function of Pard6γb in neurocoel formation is not completely shared with the other members of the zebrafish Pard6 family.

Pard6α

In order to further investigate the partial rescue of *pard6γb*^{s441} mutants with *pard6α* mRNA, we genotyped all embryos from a *pard6γb*^{s441} heterozygous incross injected with *pard6α-gfp*. Pard6α rescued the brain ventricle inflation and neurocoel phenotypes in 40% of mutants (n=4/10 mutants) (data not shown). Similarly, after co-injecting *pard6α-gfp* mRNA along with the *pard6γb* morpholino into wildtype embryos, only 58% (n=35/60) of the injected embryos exhibited collapsed brain ventricles. If Pard6α and Pard6γb function together to regulate neurocoel formation, *pard6α* morphants might at least partially phenocopy *pard6γb*^{s441} mutants. Using a *pard6α* morpholino targeted to the first exon-intron junction, we found that *pard6α* morphants did not phenocopy *pard6γb*^{s441} mutants, although they did exhibit pericardial edema at 30 and 56 hpf (data not shown). Analysis of the neural tube of *pard6γb*^{s441} mutants injected with the *pard6α* morpholino revealed that apical membranes still formed (data not shown), although the pericardial edema was more severe than in *pard6γb*^{s441} mutants or *pard6α* morphants. Thus, while overexpression of Pard6α can partially rescue the neurocoel phenotype of *pard6γb*^{s441} mutants, it appears that the zygotic expression of *pard6α* does not play a primary/direct role in neurocoel formation. Of course, it remains possible that maternal supplies of Pard6α protein and/or *pard6α* mRNA play a role in this process.

Discussion

In this paper, we report the isolation of a *pard6γb* mutation in zebrafish and analyze the resulting phenotypes. In addition to the phenotypes previously observed in embryos defective for components of the polarity machinery, *pard6γb*^{s441} mutants exhibit a distinct neural tube phenotype. We used this neural tube phenotype to investigate the extent of functional redundancy between the four Pard6 proteins as well as the role of the protein-protein interaction domains in Pard6γb localization and function. Our analyses of the first vertebrate mutation in a *pard6* gene highlight the functional diversity of the Par6 protein family and should facilitate future analyses of this family in vertebrate systems.

Neurocoel morphogenesis

The multiple lumen phenotype we describe in *pard6γb*^{s441} mutant neural tubes has not been reported before and is not observed in 24 hpf *has/prkci*^{m567} or *moe/epb41l5* mutants (data not shown). A defect in apical membrane formation resulting from a reduction in Pard6 function is not surprising, but the ensuing phenotype observed

in *pard6γb*^{s441} mutants, i.e. the formation of multiple small lumens, is maybe less intuitive. Indeed, this multiple lumen phenotype may be driven by the affinity of apical membranes for each other, thereby leading to small clusters of cells around a central lumen. Mpp5 might be playing additional roles required for this cellular organization, or the inflation of the lumens necessary for their easy detection. A multiple lumen phenotype has also been recently described in the gut of certain zebrafish mutants/morphants (Bagnat et al., 2007), and in that tissue, single lumen formation appears to result from the inflation and coalescence of multiple small lumens. That process may also be at play in the neural tube although the alignment of the cells on either side of the midline and the subsequent alignment of their apical membranes suggest that other mechanisms must also be involved (Belting and Affolter, 2007).

Domain analysis

Pard6 proteins are known to interact with Prkci and Cdc42 through their PB1 and partial CRIB domains, respectively. By deleting these domains, we found that the PB1 and CRIB domains are required for Pard6γb function, but dispensable for determining its subcellular localization in the neural tube at 24 hpf, indicative of redundant localization mechanisms as discussed below. The PB1 domain was first identified using human Par6 in MDCK cells (Suzuki et al., 2003). Similar to our results with zebrafish Pard6γb, deletion of this domain had no effect on subcellular localization (Suzuki et al., 2001, 2003). Also consistent with our observations of ΔPB1:GFP lacking function, overexpressing the mutant human form in MDCK cells caused a different effect than overexpressing the wildtype form (Suzuki et al., 2001, 2003).

Previous investigations using *Drosophila* embryos and MDCK cells have addressed how DmPar-6 or mammalian Pard6A function and localization are affected when these proteins cannot interact with Cdc42. Analyses in *Drosophila* suggested that without interaction with Cdc42, DmPar-6 could neither function nor localize to apical membranes (Hutterer et al., 2004). However, analysis of a similar mutant form of mammalian Pard6A in MDCK cells suggested that without Cdc42 binding, Pard6A could still localize to cell membranes just as the wildtype form (Gao and Macara, 2004). The functional results in *Drosophila* were similar to those we observed with zebrafish Pard6γb(ΔCRIB)-GFP: neither protein was functional. However, the subcellular localization of the Pard6γb(ΔCRIB)-GFP form of zebrafish Pard6γb was not altered, similar to the analysis of mammalian Pard6A. One explanation for this difference could be the presence of multiple Pard6 family members in vertebrates. Because there is only one DmPar-6 protein and *Drosophila par-6* mutants do not establish epithelial polarity (Hutterer et al., 2004), lack of Par-6 function (through deletion of the CRIB domain) in *Drosophila* embryos lacking both maternal and zygotic Par-6 would inherently lead to mislocalization. In contrast, functional redundancy between the multiple Pard6 family members in vertebrates could lead to localization of the Pard6 proteins' binding partners including Prkci, Pard3, and Nok/Mpp5. Apical localization of these proteins (through interaction with remaining Pard6 family members) could recruit the Pard6γb (ΔCRIB)-GFP form of zebrafish Pard6γb to the apical membrane. Thus, redundant mechanisms appear to regulate Pard6γb localization, but functionality requires each of the domains tested.

The Pard6 protein family

Our results provide evidence that Pard6γb represents one of four apically localized Pard6 proteins in zebrafish. All four members of the Pard6 family (Pard6α, Pard6β, Pard6γa, Pard6γb) can localize to the apical membranes in the neural tube. These data are generally consistent with the reported analysis of the three mammalian *Pard6* genes using MDCK cells. In agreement with our findings, mammalian Pard6B and Pard6C were localized primarily to the membranes of MDCK cells, overlapping with ZO-1, but mammalian Pard6A localized primarily to the cytoplasm (Gao and Macara, 2004). One explanation for the Pard6A localization discrepancy could be that the cytoplasmic localization was a result of overexpression or that it is cell type specific.

Despite their ability to localize apically, Pard6α, but not Pard6γa nor Pard6β, could partially compensate for the loss of Pard6γb function. Most surprisingly, injection of the *pard6γa* gene, which likely represents a genetic duplication of *pard6γb*, could not rescue the *pard6γb*^{s441} phenotype. To further test this result, we injected mRNA's from two different wildtype alleles of *pard6γa* that originated from two different wildtype strains. Neither of these alleles was able to rescue the *pard6γb*^{s441} mutant phenotypes. While the possibility of an undetectable partial rescue remains, it appears that Pard6γa and Pard6γb are not functionally redundant during neurocoel formation.

Most, if not all, proteins involved in apicobasal polarity in zebrafish appear to be maternally provided, through deposition of proteins or their corresponding mRNAs. The stability of these maternally deposited components will influence when phenotypes first appear in the zygotic mutants. In such a model, it is possible that *pard6γb*^{s441} mutants, but not *has/prkci*^{m567} mutants, exhibit a neural tube phenotype because neural tube cells run out of Pard6γb before they can make enough apical membranes. Alternatively, the existence of proteins with at least partially redundant functions, e.g. Pard6α or aPKCzeta, may mask or further delay the appearance of these phenotypes. Thus, maternally deposited Pard6α may function to form apical membranes in the neural tube in the absence of maternal and zygotic Pard6γb. Alternatively, Pard6 independent mechanisms might be used for apical membrane formation as in *C. elegans* (Totong et al., 2007).

Despite cross-species conservation, small variations in the PB1, CRIB, and PDZ domains may contribute to differences in function (Gao and Macara, 2004). The amino acids outside these domains most likely also contribute to unique functions or interactions. One such interaction has been found between Pard6 and TGFβ receptors (Ozdamar et al., 2005). Alternatively, each Pard6 protein could be promiscuous and protein-protein interactions could thus be modulated by the expression of tissue-specific binding partners (Bit-Avragim et al., 2008b). In combination with the disparate expression patterns of the four Pard6 family members, these data suggest that the vertebrate Pard6 proteins may regulate unique aspects of development, as previously proposed (Gao and Macara, 2004). In contrast, vertebrate genomes only encode one Pard3 protein (Wei et al., 2004; Hirose et al., 2006).

Prior to 18 hpf, the localization of Pard6γb fusion proteins to nuclei may be indicative of nuclear sequestration. Nuclear localization has also been observed for Nok/Mpp5 (Bit-Avragim et al., 2008a). This observation further supports the idea of unique temporal and spatial protein-protein interactions between Pard6 proteins and their binding partners, and suggests the existence of unappreciated means of regulating Pard6 localization. In addition, Par proteins have recently been associated with progenitor cell proliferation (Costa et al., 2008) and this role might be associated with their nuclear localization.

In agreement with previous observations (Gao and Macara, 2004), the vertebrate Pard6 proteins do not overlap in function, probably due to unique protein-protein interactions and/or subcellular localization. Zebrafish could provide a model system to further examine the functions of vertebrate Pard6 proteins *in vivo* using morpholino knockdown analysis and/or by identifying mutations in the other *pard6* genes. It will be important to analyze the unique functions of known binding partners of the Pard6 protein family *in vivo*, such as Cdc42 (Atwood et al., 2007; Martin-Belmonte et al., 2007), and identify the additional binding partners of the Pard6 protein family in vertebrates. We examined the role of one Pard6 protein in zebrafish, Pard6γb, and found that it regulates the development of epithelial

tissues. More specifically, it directs morphogenesis of the neurocoel by regulating formation of a continuous lumen along the neural tube. Further analyses of these processes and the functions of the *pard6* genes in zebrafish may help identify new mechanisms regulating apicobasal polarity and neurulation.

Acknowledgments

We would like to thank A. Ayala, S. Waldron, N. Zvenigorodsky for excellent fish care and maintenance, the Alexander M. Reugels laboratory for Pard3-GFP and the Scott Fraser laboratory for the H2B-mRFP construct. H. Field, C. Shin, and M. Bagnat for screening, F. Del Bene and the Geraldine Seydoux laboratory for assistance with fusion protein design, K. Thorn and the Nikon Imaging Center for microscope use and expertise, D. Apollon, M. Bagnat, I. Cheung, S. Curado, S. Horne, A. Wehman, C. Yin, D. Bilder and reviewers for discussions and/or critical comments on the manuscript. C.A.M. was an NSF predoctoral fellow. J.H. is, and H.V. was, a long-term fellow of the Human Frontier Science Program Organization (HFSPO). This work was supported in part by grants from the NIH (NIDDK) and the Packard Foundation to D.Y.R.S.

Appendix A. Supplementary data

Supplementary data associated with this article can be found, in the online version, at doi:10.1016/j.ydbio.2008.08.033.

References

Alexander, J., Stainier, D.Y., Yelon, D., 1998. Screening mosaic F1 females for mutations affecting zebrafish heart induction and patterning. Dev. Genet. 22, 288–299.

Atwood, S.X., Chabu, C., Penkert, R.R., Doe, C.Q., Prehoda, K.E., 2007. Cdc42 acts downstream of Bazooka to regulate neuroblast polarity through Par-6 aPKC. J. Cell. Sci. 120, 3200–3206.

Bagnat, M., Cheung, I.D., Mostov, K.E., Stainier, D.Y., 2007. Genetic control of single lumen formation in the zebrafish gut. Nat. Cell Biol. 9, 954–960.

Belting, H.G., Affolter, M., 2007. It takes guts to make a single lumen. Nat. Cell Biol. 9, 880–881.

Bit-Avragim, N., Rohr, S., Rudolph, F., Van Der Ven, P., Furst, D., Eichhorst, J., Wiesner, B., Abdelilah-Seyfried, S., 2008a. Nuclear localization of the zebrafish tight junction protein Nagie oko. Dev. Dyn. 237, 83–90.

Bit-Avragim, N., Hellwig, N., Rudolph, F., Munson, C., Stainier, D.Y., Abdelilah-Seyfried, S., 2008b. Divergent polarization mechanisms during vertebrate epithelial development mediated by the Crumbs complex protein Nagie oko. J. Cell. Sci. 121, 2503–2510.

Christensen, A.K., Jensen, A.M., 2008. Tissue-specific requirements for specific domains in the FERM protein Moe/Epb4.1l5 during early zebrafish development. BMC Dev. Biol. 8, 3.

Ciruna, B., Jenny, A., Lee, D., Mlodzik, M., Schier, A.F., 2006. Planar cell polarity signalling couples cell division and morphogenesis during neurulation. Nature 439, 220–224.

Costa, M.R., Wen, G., Lepier, A., Schroeder, T., Gotz, M., 2008. Par-complex proteins promote proliferative progenitor divisions in the developing mouse cerebral cortex. Development 135, 11–22.

Etemad-Moghadam, B., Guo, S., Kemphues, K.J., 1995. Asymmetrically distributed PAR-3 protein contributes to cell polarity and spindle alignment in early C. elegans embryos. Cell 83, 743–752.

Gao, L., Macara, I.G., 2004. Isoforms of the polarity protein par6 have distinct functions. J. Biol. Chem. 279, 41557–41562.

Garrard, S.M., Capaldo, C.T., Gao, L., Rosen, M.K., Macara, I.G., Tomchick, D.R., 2003. Structure of Cdc42 in a complex with the GTPase-binding domain of the cell polarity protein, Par6. Embo. J. 22, 1125–1133.

Geldmacher-Voss, B., Reugels, A.M., Pauls, S., Campos-Ortega, J.A., 2003. A 90-degree rotation of the mitotic spindle changes the orientation of mitoses of zebrafish neuroepithelial cells. Development 130, 3767–3780.

Gibson, M.C., Perrimon, N., 2003. Apicobasal polarization: epithelial form and function. Curr. Opin. Cell Biol. 15, 747–752.

Gotta, M., Abraham, M.C., Ahringer, J., 2001. CDC-42 controls early cell polarity and spindle orientation in C. elegans. Curr. Biol. 11, 482–488.

Gotz, M., Huttner, W.B., 2005. The cell biology of neurogenesis. Nat. Rev. Mol. Cell Biol. 6, 777–788.

Guo, S., Kemphues, K.J., 1995. par-1, a gene required for establishing polarity in C. elegans embryos, encodes a putative Ser/Thr kinase that is asymmetrically distributed. Cell 81, 611–620.

Hirose, T., Karasawa, M., Sugitani, Y., Fujisawa, M., Akimoto, K., Ohno, S., Noda, T., 2006. PAR3 is essential for cyst-mediated epicardial development by establishing apical cortical domains. Development 133, 1389–1398.

Hong, E., Brewster, R., 2006. N-cadherin is required for the polarized cell behaviors that drive neurulation in the zebrafish. Development 133, 3895–3905.

Horne-Badovinac, S., Lin, D., Waldron, S., Schwarz, M., Mbamalu, G., Pawson, T., Jan, Y., Stainier, D.Y., Abdelilah-Seyfried, S., 2001. Positional cloning of heart and soul reveals multiple roles for PKC lambda in zebrafish organogenesis. Curr. Biol. 11, 1492–1502.

Horne-Badovinac, S., Rebagliati, M., Stainier, D.Y., 2003. A cellular framework for gut-looping morphogenesis in zebrafish. Science 302, 662–665.

Huisken, J., Swoger, J., Del Bene, F., Wittbrodt, J., Stelzer, E.H., 2004. Optical sectioning deep inside live embryos by selective plane illumination microscopy. Science 305, 1007–1009.

Hurd, T.W., Gao, L., Roh, M.H., Macara, I.G., Margolis, B., 2003. Direct interaction of two polarity complexes implicated in epithelial tight junction assembly. Nat. Cell Biol. 5, 137–142.

Hutterer, A., Betschinger, J., Petronczki, M., Knoblich, J.A., 2004. Sequential roles of Cdc42, Par-6, aPKC, and Lgl in the establishment of epithelial polarity during Drosophila embryogenesis. Dev. Cell 6, 845–854.

Jensen, A.M., Westerfield, M., 2004. Zebrafish mosaic eyes is a novel FERM protein required for retinal lamination and retinal pigmented epithelial tight junction formation. Curr. Biol. 14, 711–717.

Joberty, G., Petersen, C., Gao, L., Macara, I.G., 2000. The cell-polarity protein Par6 links Par3 and atypical protein kinase C to Cdc42. Nat. Cell Biol. 2, 531–539.

Johnson, S.L., Gates, M.A., Johnson, M., Talbot, W.S., Horne, S., Baik, K., Rude, S., Wong, J.R., Postlethwait, J.H., 1996. Centromere-linkage analysis and consolidation of the zebrafish genetic map. Genetics 142, 1277–1288.

Kramer-Zucker, A.G., Wiessner, S., Jensen, A.M., Drummond, I.A., 2005. Organization of the pronephric filtration apparatus in zebrafish requires Nephrin, Podocin and the FERM domain protein Mosaic eyes. Dev. Biol. 285, 316–329.

Lin, D., Edwards, A.S., Fawcett, J.P., Mbamalu, G., Scott, J.D., Pawson, T., 2000. A mammalian PAR-3-PAR-6 complex implicated in Cdc42/Rac1 and aPKC signalling and cell polarity. Nat. Cell Biol. 2, 540–547.

Lowery, L.A., Sive, H., 2004. Strategies of vertebrate neurulation and a re-evaluation of teleost neural tube formation. Mech. Dev. 121, 1189–1197.

Lowery, L.A., Sive, H., 2005. Initial formation of zebrafish brain ventricles occurs independently of circulation and requires the nagie oko and snakehead/atp1a1a.1 gene products. Development 132, 2057–2067.

Martin-Belmonte, F., Gassama, A., Datta, A., Yu, W., Rescher, U., Gerke, V., Mostov, K., 2007. PTEN-mediated apical segregation of phosphoinositides controls epithelial morphogenesis through Cdc42. Cell 128, 383–397.

Megason, S.G., Fraser, S.E., 2003. Digitizing life at the level of the cell: high-performance laser-scanning microscopy and image analysis for in toto imaging of development. Mech. Dev. 120, 1407–1420.

Neff, M.M., Turk, E., Kalishman, M., 2002. Web-based primer design for single nucleotide polymorphism analysis. Trends Genet. 18, 613–615.

Ober, E.A., Verkade, H., Field, H.A., Stainier, D.Y., 2006. Mesodermal Wnt2b signalling positively regulates liver specification. Nature 442, 688–691.

Omori, Y., Malicki, J., 2006. oko meduzy and related crumbs genes are determinants of apical cell features in the vertebrate embryo. Curr. Biol. 16, 945–957.

Ozdamar, B., Bose, R., Barrios-Rodiles, M., Wang, H.R., Zhang, Y., Wrana, J.L., 2005. Regulation of the polarity protein Par6 by TGFbeta receptors controls epithelial cell plasticity. Science 307, 1603–1609.

Papan, C., Campos-Ortega, J.A., 1999. Region-specific cell clones in the developing spinal cord of the zebrafish. Dev. Genes Evol. 209, 135–144.

Peterson, R.T., Mably, J.D., Chen, J.N., Fishman, M.C., 2001. Convergence of distinct pathways to heart patterning revealed by the small molecule concentramide and the mutation heart-and-soul. Curr. Biol. 11, 1481–1491.

Petronczki, M., Knoblich, J.A., 2001. DmPAR-6 directs epithelial polarity and asymmetric cell division of neuroblasts in Drosophila. Nat. Cell Biol. 3, 43–49.

Qiu, R.G., Abo, A., Steven Martin, G., 2000. A human homolog of the C. elegans polarity determinant Par-6 links Rac and Cdc42 to PKCzeta signaling and cell transformation. Curr. Biol. 10, 697–707.

Reugels, A.M., Boggetti, B., Scheer, N., Campos-Ortega, J.A., 2006. Asymmetric localization of Numb:EGFP in dividing neuroepithelial cells during neurulation in Danio rerio. Dev. Dyn. 235, 934–948.

Rodriguez-Boulan, E., Nelson, W.J., 1989. Morphogenesis of the polarized epithelial cell phenotype. Science 245, 718–725.

Rohr, S., Bit-Avragim, N., Abdelilah-Seyfried, S., 2006. Heart and soul/PRKCi and Nagie oko/Mpp5 regulate myocardial coherence and remodeling during cardiac morphogenesis. Development 133, 107–115.

Shu, X., Shaner, N.C., Yarbrough, C.A., Tsien, R.Y., Remington, S.J., 2006. Novel chromophores and buried charges control color in mFruits. Biochemistry 45, 9639–9647.

Suzuki, A., Ohno, S., 2006. The PAR-aPKC system: lessons in polarity. J. Cell. Sci. 119, 979–987.

Suzuki, A., Yamanaka, T., Hirose, T., Manabe, N., Mizuno, K., Shimizu, M., Akimoto, K., Izumi, Y., Ohnishi, T., Ohno, S., 2001. Atypical protein kinase C is involved in the evolutionarily conserved par protein complex and plays a critical role in establishing epithelia-specific junctional structures. J. Cell Biol. 152, 1183–1196.

Suzuki, A., Akimoto, K., Ohno, S., 2003. Protein kinase C lambda/iota (PKClambda/iota): a PKC isotype essential for the development of multicellular organisms. J. Biochem. (Tokyo) 133, 9–16.

Tawk, M., Araya, C., Lyons, D.A., Reugels, A.M., Girdler, G.C., Bayley, P.R., Hyde, D.R., Tada, M., Clarke, J.D., 2007. A mirror-symmetric cell division that orchestrates neuroepithelial morphogenesis. Nature 446 (7137) (Apr 12), 797–800.

Thisse, B., Pflumio, S., Fürthauer, M., Loppin, B., Heyer, V., Degrave, A., Woehl, R., Lux, A., Steffan, T., Charbonnier, X.Q. and Thisse, C. (2001) Expression of the zebrafish

genome during embryogenesis (NIH R01 RR15402). ZFIN Direct Data Submission (http://zfin.org).
Totong, R., Achilleos, A., Nance, J., 2007. PAR-6 is required for junction formation but not apicobasal polarization in C. elegans embryonic epithelial cells. Development 134, 1259–1268.
Ueno, N., Greene, N.D., 2003. Planar cell polarity genes and neural tube closure. Birth Defects Res. C. Embryo. Today 69, 318–324.
von Trotha, J.W., Campos-Ortega, J.A., Reugels, A.M., 2006. Apical localization of ASIP/PAR-3:EGFP in zebrafish neuroepithelial cells involves the oligomerization domain CR1, the PDZ domains, and the C-terminal portion of the protein. Dev. Dyn. 235, 967–977.
Wang, Q., Hurd, T.W., Margolis, B., 2004. Tight junction protein Par6 interacts with an evolutionarily conserved region in the amino terminus of PALS1/stardust. J. Biol. Chem. 279, 30715–30721.
Watts, J.L., Etemad-Moghadam, B., Guo, S., Boyd, L., Draper, B.W., Mello, C.C., Priess, J.R., Kemphues, K.J., 1996. par-6, a gene involved in the establishment of asymmetry in early C. elegans embryos, mediates the asymmetric localization of PAR-3. Development 122, 3133–3140.
Wei, X., Malicki, J., 2002. nagie oko, encoding a MAGUK-family protein, is essential for cellular patterning of the retina. Nat. Genet. 31, 150–157.
Wei, X., Cheng, Y., Luo, Y., Shi, X., Nelson, S., Hyde, D.R., 2004. The zebrafish Pard3 ortholog is required for separation of the eye fields and retinal lamination. Dev. Biol. 269, 286–301.
Westerfield, M., 1995. The Zebrafish Book: A Guide for the Laboratory Use of Zebrafish (Brachydanio rerio). Eugene, OR: University of Oregon Press.
Yelon, D., Horne, S.A., Stainier, D.Y., 1999. Restricted expression of cardiac myosin genes reveals regulated aspects of heart tube assembly in zebrafish. Dev. Biol. 214, 23–37.